Control Engineering Practice 18 (2010) 665–675

Contents lists available at ScienceDirect

Control Engineering Practice

journal homepage: www.elsevier.com/locate/conengprac

Optimal switching control of burner setting for a compact marine boiler design

Brian Solberg [a,*], Palle Andersen [b], Jan M. Maciejowski [c], Jakob Stoustrup [b]

[a] DONG Energy, A. C. Meyers Vænge 9, 2450 København SV, Denmark
[b] Department of Electronic Systems, Aalborg University, Fredrik Bajers Vej 7C, 9220 Aalborg Øst, Denmark
[c] Department of Engineering, University of Cambridge, Trumpington Street, Cambridge CB2 1PZ, UK

ARTICLE INFO

Article history:
Received 13 March 2008
Accepted 16 March 2010

Keywords:
Marine boiler
Hybrid systems
Hysteresis control
Model predictive control
Limit cycles

ABSTRACT

This paper discusses optimal control strategies for switching between different burner modes in a novel compact marine boiler design. The ideal behaviour is defined in a performance index the minimisation of which defines an ideal trade-off between deviations in boiler pressure and water level from their respective setpoints and the cost of burner switches and variation of continuous input flows. Direct minimisation was found computationally infeasible and two different suboptimal strategies have been considered. The first one is based on the mixed logical dynamical framework. The second approach is based on a generalisation of hysteresis control. The strategies are verified on a simulation model of the compact marine boiler for control of low/high burner load switches.

1. Introduction

The control of marine boilers mainly focuses on minimising the variation of steam pressure and water level in the boiler, keeping both variables around some given setpoint. Up till now this task has been achieved using classical single input single output controllers, one using the fuel flow to control the steam pressure and one using the feed water flow to control the water level.

A more efficient control can allow smaller water and steam volumes in the boiler implying lower production and running costs and a more attractive product. In Solberg, Karstensen, Andersen, Pedersen, and Hvistendahl (2005) a successful application of LQG control to the MISSION™ OB boiler from Aalborg Industries A/S product range was shown.

The specific boiler concerned in the present work is a novel compact marine boiler from Aalborg Industries A/S. The boiler is a side-fired one-pass smoke tube boiler. The boiler consists of a furnace and convection tubes surrounded by water. At the top of the boiler steam is led out and feed water is injected. The compact boiler is equipped with a two-stage burner unit with two pressure atomiser nozzles of different size. This unit is under development and not all details can be revealed here, but of significance for the control is that under medium and high load both burners must be used, at low load Burner 2 (the largest nozzle) may be turned off, but Burner 1 (the smallest nozzle) must be on whenever Burner 2 is on. This allows a high turn-down ratio, defined as the ratio between the highest and lowest possible fuel flow or equivalently burner heating power. However, the configuration considered in this paper leaves a gap between the maximum power from Burner 1 and the minimum power from Burner 1 plus Burner 2. This gap may be compensated through intelligent switching respecting safety and trading deviations in pressure and water level against increased actuator wear and non-optimal combustion during burner start-up. A similar switching strategy may also expand the turn-down ratio below the minimum power of Burner 1 alone.

The challenge in this work is to design an appropriate burner switching strategy that minimises pressure variations and hence fluctuations in steam quality without compromising water level performance to still allow the smaller boiler geometry. Such a task would normally have been approached using heuristic rules combined with hysteresis control, however, a more systematic design procedure is sought.

The control of boilers has been undergoing intensive research over the years. Especially for control of the continuous parts of the dynamics many advanced methods have been proposed—see e.g. Mortensen, Mølbak, Andersen, and Pedersen (1998), Zhao, Li, Taft, and Bentsman (1999), Lee, Kwon, and Kwon (2000), Kothare, Mettler, Morari, Bendotti, and Falinower (2000), and Rossiter, Neal, and Yao (2002).

Unlike most previous work on boiler control the challenge here requires integration of logic and dynamics and especially handling of discrete inputs. Many methods have been proposed for controlling such hybrid systems. Many of these are based on on-line optimisation schemes—see e.g. Sarabia, de Prada, Cristea,

* Corresponding author.
E-mail address: brsol@dongenergy.dk (B. Solberg).

0967-0661/$ - see front matter © 2010 Elsevier Ltd. All rights reserved.
doi:10.1016/j.conengprac.2010.03.009

and Mazaeda (2005), Bemporad and Morari (1999), and Hedlund and Rantzer (1999). Others, such as traditional hysteresis control, are based on conditional switching. For systems whose optimal state trajectory converge to a limit cycle, a generalisation of hysteresis control was presented in Solberg, Andersen, and Stoustrup (2008) given only discrete decision variable. In Giua, Seatzu, and Van der Mee (2001), Xuping and Antsaklis (2003), and Seatzu, Corona, Giua, and Bemporad (2006) the authors treat switched linear and affine systems. It is noted that when the switching sequence is predetermined the optimal control reduces to a state feedback. However, the focus is restricted to a finite number of switches. In relation to boiler control there are a few examples of hybrid control and these often focus on handling load varying dynamics—see e.g. Keshavarz, Barkhordary, and Motlagh (2007) and Cheng, Bentsman, and Taft (2008).

In this paper optimality is defined with respect to minimisation of the performance index, penalising pressure and water level setpoint deviations and control actions, while including a penalty on burner switches and related additional fuel use. Two different suboptimal control strategies shall be compared:

- The first strategy, Method A, described in Solberg, Andersen, Maciejowski, and Stoustrup (2008) uses finite horizon model predictive control (MPC) in combination with the mixed logical dynamical (MLD) framework (Bemporad & Morari, 1999) which is an approach where standard tools can be applied to obtain an optimising control law. In Solberg, Andersen, Maciejowski, et al. (2008) this method was compared to an MPC combined with traditional hysteresis control.
- The second strategy, Method B, uses a cascade control configuration where a generalised hysteresis controller sends functions describing switching surfaces for the hysteresis, calculated from an infinite horizon optimisation problem, to an inner loop. Method B is the only strategy known to the authors which allows an infinite number of switches while penalising switches in the cost function.

It is shown through simulations that Method B in general produces better responses than Method A. The main reason for this is argued to be the mismatch between predicted and real switches due to blocking of switches and a relatively short prediction horizon both introduced in Method A to make the computations feasible. Method B is further found computationally more attractive than Method A for on-line implementation.

The paper is organised as follows: First the marine boiler system is introduced and control properties of this are discussed. Second the two suboptimal control strategies are discussed. In the subsequent section these two methods are compared in a simulation study. Finally conclusion and future works are presented.

2. System description

The boiler consists of two logically separated parts, one containing the heating system and one containing the water–steam system. The heating system consists of the furnace and the convection tubes. The water–steam system consists of all water and steam in the boiler. These two systems are interconnected by the metal separating them i.e. the furnace jacket and the convection tube jackets.

The boiler is equipped with two actuator systems for feed water and burner control, respectively. The feed water flow dynamics are linearised in an inner cascade controller which allows the reference to the feed water flow to be used as a manipulated variable. The corresponding inner loop can easily be designed to be faster than the outer loop. The burner system is more complicated. It can operate in three modes; Mode 0: both burners off; Mode 1: Burner 1 on and Burner 2 off; Mode 2: both burners on. A sketch of the boiler system is shown in Fig. 1.

The function of the burner unit can be described by a finite state machine. The state machine consists of six states: three representing the modes described above and another three describing transitions between these, see Fig. 2.

The function of each state is summarised in Table 1.

States n_1, n_2 are characterised by the continuous input variable, fuel, $\dot{m}_{fu}$, being controllable. In contrast transition states $n_{0,1}$, $n_{1,2}$, $n_{1,0}$ are governed by predetermined control sequences. To initiate a switch between modes, certain guards have to be satisfied, as shown in Fig. 2. In most cases this is just a matter of setting the Boolean variable, $u_{b,1}$ or $u_{b,2}$, corresponding to the specific burner being on or off. However, to initiate a switch from Mode 1 to Mode 2, $n_1 \rightarrow n_{1,2}$, the combustion air flow and hence the fuel flow to Burner 1 has to be below a certain level, $\underline{\dot{m}}_{fu}^{1,2}$, in order to be able to fire Burner 2.

In the boiler design considered in this paper the maximum power generated by Burner 1, $\overline{Q}_l$, alone is lower than the minimum power generated by the combined operation of the burners, $\underline{Q}_h$. This is illustrated in Fig. 3 where the shaded area corresponds to possible power inputs. There are two power gaps in the figure. This means that, for a steam flow that corresponds to a steady state power consumption, Q_{ss}, in one of these gaps, the burners have to follow some on/off switching scheme to keep the pressure around its reference value. The gaps will be defined as: *Gap-region* 1 $Q_{ss} \in [0; \underline{Q}_l] := G_1 \subset \mathbb{R}$ and *Gap-region* 2 $Q_{ss} \in [\overline{Q}_l; \underline{Q}_h] := G_2 \subset \mathbb{R}$. In the sequel these gap-regions are referred to a bit loosely using statements such as 'the disturbance-', 'the required fuel flow-', 'the power request belong to a gap-region', which all translate into the equivalent formulation that the steady state power consumption cannot be met exactly by any available fuel flow. In other designs and fuel systems Gap-region 2 is not present. In this case the methods proposed are still relevant in order to deliver low steam flow below $\underline{Q}_l$ and thus large turn-down ratio.

2.1. Modelling

A simplified burner model consists of the state machine shown in Fig. 2. The model should describe the total fuel supply to the two burners $\dot{m}_{fu} = \dot{m}_{fu,1} + \dot{m}_{fu,2}$ as this is assumed equivalent to the total power delivered from the burner unit. This model is different for each state in the finite state machine. In the transition states $n_{0,1}$, $n_{1,2}$, $n_{1,0}$ the fuel flow is constrained to move according to certain patterns. In n_0 there is no flow. In n_1 the fuel flow is equal to the flow to Burner 1. Finally in n_2 an underlying controller distributes the fuel and combustion air flow references to the two burners in order to maximise efficiency while keeping a clean combustion with an oxygen percentage of the exhaust gas above three percent. The total fuel flow can be assumed to be equal to the reference due to the much faster dynamics of the combustion process than that of the boiler water–steam part. Note here that the fuel flow rate constraints are different in n_1 and n_2.

The detailed 8th order model of the boiler presented in Solberg et al. (2005) has been simplified in Solberg, Andersen, Maciejowski, et al. (2008). This simplified model consists of three differential equations, derived from mass and energy balances, describing the pressure p_s, the water volume V_w and the volume of steam bubbles below the water surface V_b. The three differential equations are summarised as

$$\left[(V_t - V_w)\frac{d\rho_s}{dp_s} + V_w\frac{d\rho_w}{dp_s}\right]\frac{dp_s}{dt} + (\rho_w - \rho_s)\frac{dV_w}{dt} = \dot{m}_{fw} - \dot{m}_s \tag{1a}$$

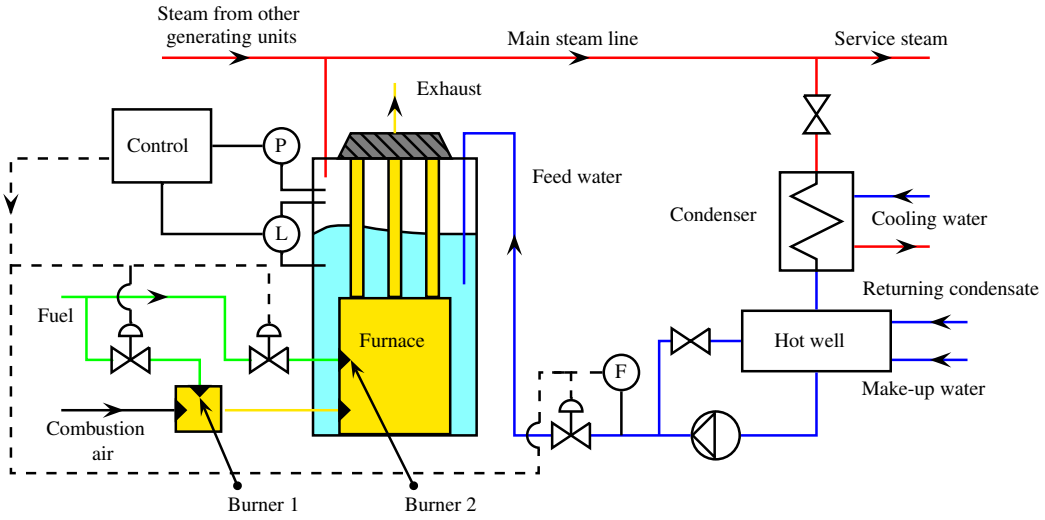

Fig. 1. Compact marine boiler principle.

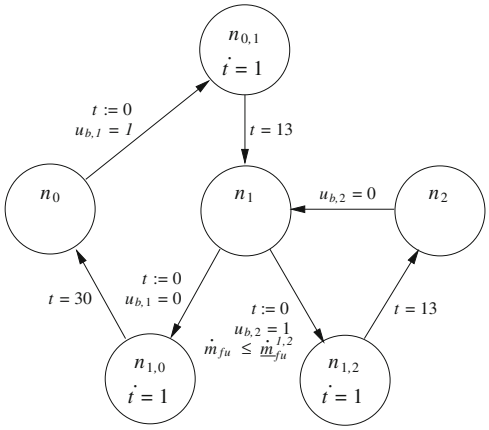

Fig. 2. Finite state machine describing burner operation.

Table 1
Description of states in the finite state machine modelling the burner unit.

n_0	*Idle*: both burners are off and Burner 1 is ready to enter start-up sequence
$n_{0,1}$	*Burner* 1 *start-up*: this state contains a sequence of events split into three time intervals. It takes 3 s from the electrode is ignited to the solenoid valve opens. Then the flame scanner must detect a flame within the next 5 s and finally the flame has 5 s to stabilise before release for modulation
n_1	*Low load*: Burner 1 is on and Burner 2 is off
$n_{1,2}$	*Burner* 2 *start-up*: this state is analogous to $n_{0,1}$
n_2	*High load*: both burners are on
$n_{1,0}$	*Shut down*: in this state Burner 1 is shut off followed by 30 s of purging

$$\left(\rho_w V_w \frac{dh_w}{dp_s} + h_w V_w \frac{d\rho_w}{dp_s} + \rho_s (V_t - V_w)\frac{dh_s}{dp_s} + h_s (V_t - V_w)\frac{d\rho_s}{dp_s} - V_t + \rho_m V_m c_{p,m}\frac{dT_s}{dp_s}\right)\frac{dp_s}{dt} + (h_w\rho_w - h_s\rho_s)\frac{dV_w}{dt} = Q + h_{fw}\dot{m}_{fw} - h_s\dot{m}_s \tag{1b}$$

$$\left((1-\beta)V_w\frac{d\rho_w}{dp_s} + V_b\frac{d\rho_s}{dp_s}\right)\frac{dp_s}{dt} + (1-\beta)\rho_w\frac{dV_w}{dt} + \rho_s\frac{dV_b}{dt} = (1-\beta)\dot{m}_{fw} - \gamma\frac{V_b}{V_w} \tag{1c}$$

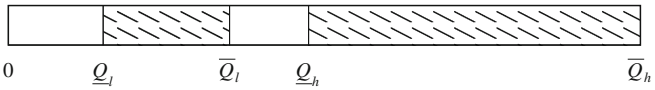

Fig. 3. Modes of operation for the two-stage burner module.

where $\dot{m}_{fw}$ is the feed water flow, $\dot{m}_s$ is the steam flow, ρ is the density, h is the enthalpy and T is the temperature, c_p is the specific heat capacity, V_t is the total volume of the boiler water–steam part and subscript m stands for metal, w for water and s for steam. γ and β are constants related to an expression describing the amount of steam escaping the water surface.

The power delivered to the water–steam part is modelled as

$$Q = \eta\dot{m}_{fu} \tag{2}$$

where η is directly dependent on the caloric value of the fuel. In addition, the proportion of the released energy which is transferred to the water side depends on the boiler load. In this context it suffices to consider η to be constant since efficiency of the heat transfer only changes modestly with load and the caloric value is constant for a given fuel. Modest changes in η only represent changes in a gain and will not change the dominating behaviour of the boiler.

In practice the water-steam circuit is closed and the steam flow is governed by several valves combined with pipe resistance. Therefore, a variable $k(t)$ expressing pipe conductance and valve strokes is introduced. $\dot{m}_s$ is then given as

$$\dot{m}_s(t) = k(t)\sqrt{p_s(t) - p_{dws}} \tag{3}$$

where the downstream pressure, p_{dws}, is the pressure in the feed water tank which is open and hence has ambient pressure, $p_{dws} = p_a$. $p_s(t) - p_{dws}$ is the differential pressure over the steam supply line. Although this is only a rough model of the flow, it is used since the flow in general is also determined by unknown user behaviour and it is thought to be preferable not to consider the flow to be independent of pressure.

The final model has the form

$$\mathbf{F}(\check{\mathbf{x}})\dot{\check{\mathbf{x}}} = \mathbf{h}(\check{\mathbf{x}}, \check{\mathbf{u}}, \check{d}) \tag{4}$$

where $\check{\mathbf{x}} = [p_s, V_w, V_b]^T$, $\check{\mathbf{u}} = [\dot{m}_{fu}, \dot{m}_{fw}]^T$ and $\check{d} = k$. The temperature of the feed water is assumed constant and therefore not included in $\check{d}$. The water level is given as: $L_w = (V_w + V_b - V_o)/A_{ws}$ (the water level is measured from the furnace top, V_o is the volume surrounding the furnace, and A_{ws} is the water surface area).

A linear approximation of (4) can be generated for controller design. In Solberg, Karstensen, and Andersen (2007) it was shown that the dynamics of the one-pass smoke tube boilers from AI, around the crossover frequency has little dependency on the steam load. For this reason it suffices to focus on a controller design derived from one linear model hence leaving out any gain scheduling. Thus the sampled linear approximation of the marine boiler takes the form

$$\check{\mathbf{x}}(k+1)=\check{\mathbf{A}}\check{\mathbf{x}}(k)+\check{\mathbf{B}}\check{\mathbf{u}}(k)+\check{\mathbf{B}}_d\check{d}(k) \tag{5a}$$

$$\check{\mathbf{y}}(k)=\check{\mathbf{C}}\check{\mathbf{x}}(k) \tag{5b}$$

$$\check{\mathbf{x}}\in\mathcal{X},\quad \check{\mathbf{u}}\in\mathcal{U}_{i(k)},\ i(k)\in\{0,1,2\} \tag{5c}$$

where i is the current burner mode, $\check{\mathbf{y}}=[p_s,L_w]^T$, $\mathcal{X}\subset\mathbb{R}^n$ and $\mathcal{U}_i\subset\mathbb{R}^m$ are compact sets describing constraints on state and inputs respectively.

2.2. Control properties

For the marine boilers concerned the well-known shrink-and-swell phenomenon from feed water flow to water level, (Åström & Bell, 2000), has not been observed in measurements. This means that this loop, in principle, is limited in bandwidth only by actuators and sensors (and model uncertainty).

Another property of the system is the high bandwidth in the response from the steam flow disturbance to the outputs. This complicates the controller design as it sets a requirement for a high closed loop bandwidth in order to suppress the effect of the disturbance. This means that the controller update frequency should be high limiting the time available between updates for on-line controller computations. In particular, the controller sampling time is set to $T_s=1$ s.

Regarding the control structure, it would be preferred to leave the burner switching to an underlying burner control system which delivers the requested fuel flow. However, due to the long sequences associated with burner stop/start both pressure and water level control are disturbed making this approach less suitable. This requires the burner switches to be handled by the pressure and water level controller.

One drawback of this strategy is that when switching from high to low load the total fuel flow becomes uncertain, as the distribution of fuel between the two burners is not modelled. Burner 2 is constrained only to turn off when the fuel flow is at a minimum, in order to avoid cutting off an unknown fuel flow in future predictions.

The control problem is formulated as follows:

Problem 1. At every sample instant k, given the current state $\check{\mathbf{x}}(k)$, minimise the following performance index over $\check{\mathbf{u}}_N^T=[\check{\mathbf{u}}(k)^T,\check{\mathbf{u}}(k+1|k)^T,\ldots]$:

$$\begin{aligned}J(\check{\mathbf{x}}(k),\check{\mathbf{u}}_N)=\lim_{N\to\infty}\frac{1}{N}\Bigg\{&\sum_{j=1}^{M(N)}h_{i_{j-1},i_j}\\&+T_s\sum_{j=0}^{N}[(\check{\mathbf{r}}(j+k|k)-\check{\mathbf{y}}(j+k|k))^T\check{\mathbf{Q}}(j)(\check{\mathbf{r}}(j+k|k)-\check{\mathbf{y}}(j+k|k))\\&+\Delta\check{\mathbf{u}}(j+k|k)^T\check{\mathbf{R}}(j)\Delta\check{\mathbf{u}}(j+k|k)]\Bigg\}\end{aligned} \tag{6}$$

where $\Delta\check{\mathbf{u}}(j)=\check{\mathbf{u}}(j)-\check{\mathbf{u}}(j-1)$, $\check{\mathbf{r}}(j)$ is the reference vector, $i\in\{0,1,2\}$, $M(N)$ is the total number of burner switches and h_{i_{j-1},i_j} is the cost associated with a switch from burner mode i_{j-1} to mode i_j. Also $\check{\mathbf{x}}(j)$ and $\check{\mathbf{y}}(j)$ evolve according to (5). $\check{\mathbf{Q}}(j)\geq 0$ and $\check{\mathbf{R}}(j)\geq 0$ are quadratic penalties on error and input changes, respectively.

Hence the control problem poses a trade-off between output (pressure and water level) setpoint deviations and control input action including costs for burner switches. It would seem natural to include a cost on the accumulated fuel use. This, however, is not implemented. The reason is that one performance criterion is to achieve zero steady state errors for both water level and pressure, when possible. A weight on the accumulated fuel use will urge the system to save fuel at the expense of inferior pressure performance. Transients including burner switches will lead to reduced efficiency implying increased fuel consumption. This is taken care of in the performance function in the weighting of input changes and burner switches.

An important property of the performance (6) is that, dependent on the choice of weights, there may exist constant steam flows corresponding to the gap-regions shown in Fig. 3, for which the cost of allowing a constant offset in the output is larger than that of introducing a limit cycle through switching the input. This would always be the case if (6) included the integral error of the pressure, as any possible constant input would result in the pressure approaching a constant value different from the setpoint, meaning that (6) would be infinite. When (6) does not include the integral error steam flows and choices of weights still exist for which the integral over one cycle of period T_p, corresponding to a switching input, will be smaller than the corresponding integral over T_p with any possible constant input and converged output. Finding the optimal limit cycle which the state trajectory converges to can be achieved by posing a relatively simple optimisation problem. The period of this limit cycle is dependent on the steam flow disturbance. The reason for this is that the steady state fuel flow required to achieve zero pressure error is dependent on the steam flow. When the required steady state fuel flow is in a gap-region and close to where the steady state solution is optimal, the limit cycle period is long because the pressure error only slowly grows to a level where the cost is comparable to the cost of switching Burner 1 or Burner 2 on and off. In the middle of the gap-region the pressure error will increase and decrease faster and the limit cycle period will be shorter.

3. Methods

In this section two suboptimal methods for solving control Problem 1 are described. The two methods are based on different control configurations. Method A incorporates both the finite state automaton and the dynamical system into one mixed integer optimisation problem (MIP) solved in a receding horizon manner. Method B exploits a strategy where an inner controller optimises over the continuous variables controlling pressure and water level. The inner controller further switches the burners when the states hit switching surfaces and an outer controller optimises over these switching surfaces.

3.1. Method A: finite horizon model predictive control

Recently discrete time finite horizon MPC has become a tractable tool for the control of hybrid systems (Bemporad & Morari, 1999). The reason is that the method offers a systematic design procedure for these systems. Modelling tools such as HYSDEL (hybrid system description language) (Torrisi & Bemporad, 2004) make it easy to generate MLD models suitable for implementation with an MPC control law. This is done by describing the system to be controlled as a discrete time hybrid automaton.

Such a procedure was in Solberg, Andersen, Maciejowski, et al. (2008) applied to the same setup as described in this paper. The strategy is illustrated in the block diagram in Fig. 4.

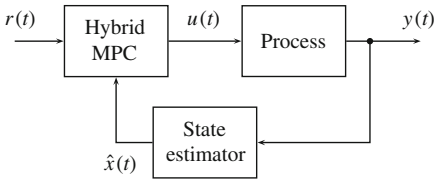

Fig. 4. Control structure for Method A.

Referring to Solberg, Andersen, Maciejowski, et al. (2008) a model of the boiler system (5) including the state machine of the burner described in HYSDEL can be put together in the MLD form using tools from the MPT-toolbox (Kvasnica, Grieder, & Baotić, 2004):

$$\mathbf{x}(k+1) = \mathbf{A}\mathbf{x}(k) + \mathbf{B}_1\mathbf{u}(k) + \mathbf{B}_2\boldsymbol{\delta}(k) + \mathbf{B}_3\mathbf{z}(k) \tag{7a}$$

$$\mathbf{y}(k) = \mathbf{C}\mathbf{x}(k) + \mathbf{D}_1\mathbf{u}(k) + \mathbf{D}_2\boldsymbol{\delta}(k) + \mathbf{D}_3\mathbf{z}(k) \tag{7b}$$

$$\mathbf{E}_2\boldsymbol{\delta}(k) + \mathbf{E}_3\mathbf{z}(k) \le \mathbf{E}_1\mathbf{u}(k) + \mathbf{E}_4\mathbf{x}(k) + \mathbf{E}_5 \tag{7c}$$

where $\mathbf{x} \in \mathbb{R}^{n_{x_r}} \times \{0,1\}^{n_{x_b}}$, $\mathbf{u} \in \mathbb{R}^{n_{u_r}} \times \{0,1\}^{n_{u_b}}$ and $\mathbf{y} \in \mathbb{R}^{n_y}$. $\boldsymbol{\delta} \in \{0,1\}^{n_\delta}$, $\mathbf{z} \in \mathbb{R}^{n_z}$ represent Boolean and continuous auxiliary variables respectively. The real part of the state vector is composed of

$$\mathbf{x}_r(k) = [p_s(k), V_w(k), V_b(k), \dot{m}_{fu}(k-1), \dot{m}_{fw}(k-1), d_{um,1}(k), d_{um,2}(k), t(k), i(k)]^T$$

where $d_{um,1}(k)$ is an unmeasured disturbance put in the direction of the steam flow and $d_{um,2}(k)$ is an unmeasured disturbance put in the direction of the feed water flow both included to achieve offset free tracking. $t(k)$ is a timing variable used during burner switches, $i(k) \in \{0,1,2\}$ is the current burner mode implemented as a continuous variable. The real part of the input vector is given using incremental inputs as $\mathbf{u}_r(k) = \Delta\mathbf{u}(k) = [\Delta\dot{m}_{fu}(k), \Delta\dot{m}_{fw}(k)]^T$. The Boolean part of the state vector describes the burner finite state machine: $\mathbf{x}_b(k) = [n_0, n_{0,1}, n_1, n_{1,2}, n_2, n_{1,0}]^T$ (Fig. 2) and the Boolean part of the input vector represents when to initiate a manoeuvre/sequence leading to a burner switch $\mathbf{u}_b(k) = [u_{b,1}, u_{b,2}]^T$. Finally $\mathbf{y}(k) = [p_s(k), L_w(k)]^T$ and $h(k) = i(k) - i(k-1)$, with $h(k) \neq 0$ denoting a change in burner mode. Note that this is a slight abuse of the h notation from (6). For further details on the model refer to Solberg, Andersen, Maciejowski, et al. (2008).

As the infinite horizon control Problem 1 is not computationally feasible in this setup a model predictive controller was designed based on minimising the following finite horizon performance index:

$$J(\mathbf{x}(0), \mathbf{u}_N) = (\mathbf{r} - \mathbf{y}(N))^T\mathbf{P}(\mathbf{r} - \mathbf{y}(N)) + \sum_{j=0}^{N-1}[(\mathbf{r} - \mathbf{y}(j))^T\mathbf{Q}(\mathbf{r} - \mathbf{y}(j)) + \Delta\mathbf{u}(j)^T\mathbf{R}\Delta\mathbf{u}(j) + Hh(j)^2] \tag{8}$$

subject to the MLD system dynamics (7), where the current time $k=0$, $N=45$, $\mathbf{u}_N^T = [\mathbf{u}(0)^T, \ldots, \mathbf{u}(N)^T]$, and $\mathbf{Q} = \text{diag}([q_1, q_2])$, $\mathbf{R} = \text{diag}([r_1, r_2])$, and the switching cost is equal to $H = h_{0,1}/T_s = h_{1,0}/T_s = h_{1,2}/T_s = h_{2,1}/T_s$. The terminal cost $\mathbf{P}$ is set equal to $\mathbf{Q}$.

To facilitate on-line computations, blocking was used on the Boolean decision variables allowing these only to change at time 0 and 1. The optimisation is performed by a search, solving constrained optimisation problems for each choice of Boolean decision variables and finally selecting the solution with the lowest cost. The computational burden of the controller implementation reduces to solving at most 5 QP's (quadratic programs, here related to the ordinary MPC algorithm) at each sample time, 3 if both burners are on or off. Besides solving the QP's, constraint matrices for the QP's involving switches must be generated along with state estimates. Note that if no blocking had been enforced, using a standard MIQP (mixed-integer quadratic program) solver, this could worst case be forced to solve a QP corresponding to all feasible combinations of the Boolean decision variables over the prediction horizon.

Regarding the feedback, a state estimator has been constructed. This estimator can operate in all modes and is hence independent of the control strategy discussed. The estimator is designed as to achieve off-set free tracking of the pressure and water level. This is done by adding integrating disturbances to the process model in the direction of the steam load disturbance and the feed water flow—see e.g. Pannocchia and Rawlings (2003).

The above method will result in suboptimal performance with respect to the original optimisation defined in Problem 1, partly because of the use of a relatively short moving horizon, and partly because of the further simplification made by the restricted change in decision variables to the first two samples. Operating over a finite horizon is never optimal when the optimal state trajectory converges to a limit cycle, as suggested in Solberg, Andersen, and Stoustrup (2008). This is the case for the boiler system for certain power requests corresponding to the gap-regions.

3.2. Method B: generalised hysteresis control

The second method discussed is based on a method described in Solberg, Andersen, and Stoustrup (2008) for controlling systems whose optimal state trajectory converge to a limit cycle. The idea is to use this method when in the gap-regions. The strategy is illustrated in the block diagram in Fig. 5.

The idea behind this scheme is that the block named switching surface optimisation might consist of setting simple hysteresis bounds for the pressure. This architecture is especially good for the marine boiler system where the disturbance profile is limited to non-frequent steps.

The switching surface optimisation block need not run at the same sample frequency as the inner MPC loop which can allow for more computational demanding algorithms to be implemented at this level. Further the switching surface optimisation needs only be executed when the power demand corresponds to the gap-regions. This requires a power estimator to run at the fastest sample time to be able to react fast when a disturbance influences the process and brings it outside the gap-regions.

Determination of when the requested power belongs to a gap-region is done from an estimate of the steady state input needed to reject the steam flow disturbance.

$$\begin{bmatrix} \mathbf{I} - \check{\mathbf{A}} & -\check{\mathbf{B}} \\ \check{\mathbf{C}} & \mathbf{0} \end{bmatrix} \begin{bmatrix} \check{\mathbf{x}}_{ss} \\ \check{\mathbf{u}}_{ss} \end{bmatrix} = \begin{bmatrix} \check{\mathbf{B}}_{umd} & \mathbf{0} \\ \mathbf{0} & \mathbf{I} \end{bmatrix} \begin{bmatrix} \check{\mathbf{d}}_{um} \\ \check{\mathbf{r}} \end{bmatrix} \tag{9}$$

Here $\check{\mathbf{d}}_{um}$ are integrating disturbances added to the process model to achieve consistent estimates of the process output. If $\check{\mathbf{B}}_{umd} = \check{\mathbf{B}}$ the estimated steady state flow would simply be the first component of the $\check{\mathbf{d}}_{um}$ vector. It turns out that a better result is achieved with $\check{\mathbf{B}}_{umd} = [\check{\mathbf{B}}_d\ \check{\mathbf{B}}_2]$ corresponding to the direction of the steam flow disturbance and the feed water flow.

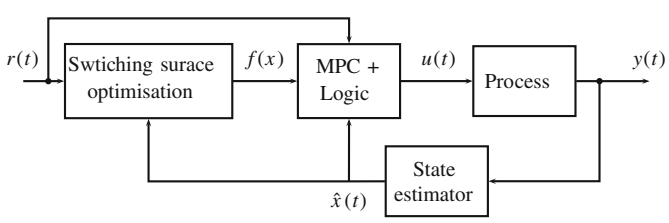

Fig. 5. Control structure for Method B.

In the following each block in Fig. 5 are described separately. The process and state estimator is equivalent to the one used in Section 3.1.

3.2.1. MPC + logic

This is the part of the controller that handles the burner switching and executes the continuous controller. The continuous controller is an MPC controller (Maciejowski, 2001; Rossiter, 2003) in which the constraints can be adjusted on-line to take into account that the fuel flow sequence executed during a switch is known. MPC control for a boiler in the same family as the one treated here is also treated in Solberg, Andersen, and Stoustrup (2007).

The performance index of the MPC controller takes the form

$$J(\check{\mathbf{x}}(0),\Delta\mathbf{u}_N)=(\mathbf{r}-\check{\mathbf{y}}(N))^T\check{\mathbf{P}}_i(\mathbf{r}-\check{\mathbf{y}}(N))+\sum_{j=0}^{N-1}[(\mathbf{r}-\check{\mathbf{y}}(j))^T\check{\mathbf{Q}}_i(\mathbf{r}-\check{\mathbf{y}}(j))+\Delta\check{\mathbf{u}}(j)^T\check{\mathbf{R}}_i\Delta\check{\mathbf{u}}(j)] \tag{10}$$

where $\check{\mathbf{Q}}_i=\check{\mathbf{P}}_i=\mathrm{diag}([\check{q}_1,\check{q}_2])$, $\check{\mathbf{R}}_i=\mathrm{diag}([\check{r}_1,\check{r}_2])$ and the index i on the weight matrices indicates the current burner mode. However, to be able to compare the two methods only one set of weights is included and these are equal to the ones for Method A. If the state belongs to a gap-region then $\check{q}_1=0$ and $\check{r}_1=\infty$. The constraints are changed according to which mode the burner unit is operating in and which sequence is executed. This is easily done by defining appropriate upper and lower bound vectors, $\underline{\Delta\mathbf{u}}$, $\overline{\Delta\mathbf{u}}$, $\underline{\mathbf{u}}$, $\overline{\mathbf{u}}$, $\underline{\mathbf{y}}$, $\overline{\mathbf{y}}$, and matrices $\mathbf{\Lambda}$, $\mathbf{\Phi}$ such that:

$$\underline{\Delta\mathbf{u}}_i(k)\le\Delta\mathbf{u}\le\overline{\Delta\mathbf{u}}_i(k),\quad \underline{\mathbf{u}}_i(k)\le\mathbf{\Lambda}\Delta\mathbf{u}\le\overline{\mathbf{u}}_i(k),\quad \underline{\mathbf{y}}\le\mathbf{\Phi}\Delta\mathbf{u}\le\overline{\mathbf{y}} \tag{11}$$

The matrices $\mathbf{\Lambda}$, $\mathbf{\Phi}$ are constant whereas the upper and lower bound vectors are changed on-line. The model used when minimising (10) over $\Delta\mathbf{u}$ subject to (11) is the same for all modes but could just as well have been different linearisations for the different load situations.

When the state hits a switching surface described in the next section a burner switch is initiated.

3.2.2. Switching surface optimisation

The final block of Fig. 5 is supposed to communicate functions describing switching surfaces to the inner MPC controller. The strategy used for this block was proposed in Solberg, Andersen, and Stoustrup (2008). In this paper two suboptimal methods for controlling systems with discrete decision variables when the optimal solution converge towards a limit cycle were proposed. One strategy was based on finding switching surface in the state space using time-optimal control related techniques to make the state converge to a predetermined limit cycle which results in a state feedback policy. Note that the approach of this section will use a continuous time linear model of the system.

Solberg, Andersen, and Stoustrup (2008) does not consider the case when there are mixed continuous and discrete decision variables. However, the authors proposed to use a sequential loop closing strategy by closing the inner loop using the continuous variables. Using sequential closing has the advantage of making the process react more intuitively to the operator. In this case the controller will attempt to regulate the water level such that it approached the reference between switches. Moreover, controlling the water level using burner switches is not of interest. The method of using the LQR state feedback to get an autonomous system was proposed in Bemporad, Giua, and Seatzu (2002). These ideas are used in the structure shown in Fig. 5. Closing the inner loop, using the MPC controller for the water level when in the gap-region, a high order linear approximation of the response from fuel to pressure can be derived. In the low frequency band this model is well approximated by the simple first order system:

$$p_s(s)=\frac{K_{p_s}}{\tau_{p_s}s+1}\dot{m}_{fu}(s) \tag{12}$$

This is the model of the system used in the outer loop for generating switching surfaces. Obvious this is only an approximation of the original setup shown in Fig. 5, which contains a constrained inner MPC controller. The performance to be minimised in this outer loop is punishing the pressure error and a continuous time equivalent to input changes. The equivalent to input changes are introduced by filtering the derivative of the input signal: $\tilde{u}_f=(1/(as+1))\dot{u}=(s/(as+1))u$ where a can be found by matching discrete time and continuous time costs. Given $z=(1/a)e^{-(1/a)t}\Delta u$ resulting from a step change in the input, leads to $\int_0^\infty rz^2\,dt=(1/T_s)r\Delta u^2\Rightarrow a=T_s/2$. As the reference is constant and the model is linearised around the desired pressure setpoint, the model of interest is

$$\begin{bmatrix}\dot{p}_s\\ \dot{u}_f\end{bmatrix}=\begin{bmatrix}-\frac{1}{\tau_{p_s}} & 0\\ 0 & -\frac{1}{a}\end{bmatrix}\begin{bmatrix}p_s\\ u_f\end{bmatrix}+\begin{bmatrix}\frac{K_{p_s}}{\tau_{p_s}}\\ 1\end{bmatrix}\dot{m}_{fu}-\begin{bmatrix}\frac{K_{p_s}}{\tau_{p_s}}\\ 0\end{bmatrix}\dot{m}_{fu,ss} \tag{13a}$$

$$\begin{bmatrix}p_s\\ \tilde{u}_f\end{bmatrix}=\begin{bmatrix}1 & 0\\ 0 & -\frac{1}{a^2}\end{bmatrix}\begin{bmatrix}p_s\\ u_f\end{bmatrix}+\begin{bmatrix}0\\ \frac{1}{a}\end{bmatrix}\dot{m}_{fu} \tag{13b}$$

where $\dot{m}_{fu,ss}$ corresponds to the steady state value of the fuel required to reject the current value of the disturbance. Recall that there are only two levels of inputs to switch between hence $\dot{m}_{fu}\in[\underline{\dot{m}}_{fu,i},\overline{\dot{m}}_{fu,i}]$ for power requests belonging to either of the gap-regions. That is: either Burner 1 is switched on and off or Burner 2 is switched on and off. However, during switches the input, $\dot{m}_{fu}$, will follow some predetermined trajectory. The cost function takes the form

$$J(\mathbf{x}(0),u_T)=\lim_{T\to\infty}\frac{1}{T}\left(\int_0^T q_1p_s^2+r_1\tilde{u}_f^2\,d\tau+\sum_{j=1}^{M(T)}h_{i_{j-1},i_j}\right) \tag{14}$$

where M is the number of burner switches and h_{i_{j-1},i_j} is the cost for switching from Mode i_{j-1} to Mode i_j. Before proceeding, recall that the task is to find switching surfaces describing the optimal limit cycle which the state converges to when minimising (14). In the meantime it might happen that no limit cycle is optimal meaning that a smaller cost is associated with allowing a constant off-set compared to tracking a limit-cycle. For this reason a dead band may be defined which redefines the gap-regions in such a way that a limit cycle is always optimal when in the gap-regions. This dead band is converted to new bounds for the gap-regions. The dead band $D\subset G$ is defined as the subset:

$$D\coloneqq\{u_{ss}|\exists u\in\{\underline{u},\overline{u}\}\wedge u_{ss}\in G\ \text{s.t.}\ J_{ss}\le J_{lc}\} \tag{15}$$

with J_{ss} being the cost for having a constant off-set and J_{lc} is the cost for staying on a limit cycle. Then the new gap is $\tilde{G}=G\backslash D$. However, when choosing an integral cost this is not possible as any constant off-set will cause the cost to become infinite. Instead a traditional dead band can be introduced in such situations:

$$D\coloneqq\{u_{ss}|\exists u\in\{\underline{u},\overline{u}\}\wedge u_{ss}\in G\ \text{s.t.}\ K_{p_s}(u-u_{ss})<\varepsilon\} \tag{16}$$

with ε being the allowed pressure error. Modifying the gap also has the effect as to provide robustness against uncertainties and noise in the steady state estimates.

The full model used in the outer loop can be described as a piece-wise affine system:

$$\dot{\mathbf{x}}(t)=\mathbf{A}_{i(t)}\mathbf{x}(t)+\mathbf{B}_{i(t)}u_{i(t)}(t)-\mathbf{B}_{d,i(t)}u_{ss}=\mathbf{A}_{i(t)}\mathbf{x}(t)+\mathbf{f}_{i(t)}(t) \tag{17a}$$

$$\mathbf{y}(t)=\mathbf{C}_{i(t)}\mathbf{x}(t)+\mathbf{D}_{i(t)}u_{i(t)}(t),\quad i(t)\in\mathcal{S} \tag{17b}$$

$$\mathbf{x}(t^+)=\mathbf{M}_{j,k}\mathbf{x}(t^-)+\mathbf{g}_{j,k} \quad \text{if } i(t^-)=j,\ i(t^+)=k \tag{17c}$$

where $i\in\mathcal{S}$ corresponding to the current burner mode and $\mathcal{S}\triangleq\{0,1,2\}$ is the different burner modes each associated with a set of model matrices. Due to the nature of the switches more than one consecutive switch at the same time instance is not allowed. The transition matrices $\mathbf{M}_{j,k}$, $\mathbf{g}_{j,k}$ are related to manoeuvres and hence do not represent instantaneous jumps in the state (here lending terminology from Frazzoli, 2001; Frazzoli, Dahleh, & Feron, 1999 where such manoeuvres made up a manoeuvre automaton for shifting between trim trajectories in helicopter flight). Instead the manoeuvres are time intervals in which the state is taken from $\mathbf{x}(t^-)$ to $\mathbf{x}(t^+)$ in time $\delta T_{j,k}$. Hence:

$$\mathbf{M}_{j,k}=e^{(\sum_{n=0}^{N-1}\mathbf{A}_{i_n}\tau_{n+1})} \tag{18a}$$

and

$$\mathbf{g}_{j,k}=\sum_{n=0}^{N-1}\left\{e^{(\sum_{h=n}^{N-1}\mathbf{A}_{i_h}\tau_{h+1})}\left[\int_0^{\tau_{n+1}}e^{-\mathbf{A}_{i_n}\tau}\mathbf{f}_{i_n}(\tau)\,d\tau\right]\right\} \tag{18b}$$

where $i_0=j$, $i_{N-1}=k$, $\delta T_{j,k}=\sum_{n=0}^{N-1}\tau_{n+1}$, $u_{j,k}(t)=\Delta\in\{u_0(\tau),\ldots,u_{N-1}(\tau)\}$ is a sequence of inputs and $\mathbf{f}_{i_n}(\tau)=\mathbf{B}_{i_n}u_n(\tau)-\mathbf{B}_{d,i_n}u_{ss}$ hence $\mathbf{g}_{j,k}$ can be split into a finite number of integrals with the same input profile e.g. a constant $u_n(t)=c$ or a ramp $u_n(t)=at+u_{n-1}$ where $t\in[0,\tau_n)$.

Now define δ_j as the time elapsed since the last input switch and corresponding manoeuvre or initial time and let T_j denote the time of the j th input switch and $M=M(T)$ the number of switches occurring in time T. The optimisation problem associated with minimising the cost (14), using the above notation, having L as the stage cost and H, h as the costs associated with switches, can be written as

$$J^*(\mathbf{x}_0)=\min_{\mathbf{T},\mathbf{I}}\lim_{T\to\infty}\frac{1}{T}\left\{\sum_{k=0}^{M(T)}[L(\mathbf{x}_k,\delta_{k+1})]+\sum_{k=1}^{M(T)}[H_{i_{k-1},i_k}(\tilde{\mathbf{x}}_k)+h_{i_{k-1},i_k}]\right\} \tag{19a}$$

s.t.

$$L(\mathbf{x}_k,\delta_{k+1})=\mathbf{x}_k^T\overline{\mathbf{Q}}_{i_k}(\delta_{k+1})\mathbf{x}_k+\mathbf{x}_k^T\overline{\mathbf{r}}_{i_k}(\delta_{k+1})+\overline{s}_{i_k}(\delta_{k+1}) \tag{19b}$$

$$H_{i_{k-1},i_k}(\tilde{\mathbf{x}}_k)=\tilde{\mathbf{x}}_k^T\overline{\mathbf{Q}}_{i_{k-1},i_k}\tilde{\mathbf{x}}_k+\tilde{\mathbf{x}}_k^T\overline{\mathbf{r}}_{i_{k-1},i_k}+\overline{s}_{i_{k-1},i_k} \tag{19c}$$

$$\tilde{\mathbf{x}}_{k+1}=\overline{\mathbf{A}}_{i_k}(\delta_{k+1})\mathbf{x}_k+\overline{\mathbf{f}}_{i_k}(\delta_{k+1}) \tag{19d}$$

$$\mathbf{x}_{k+1}=\mathbf{M}_{i_k,i_{k+1}}\tilde{\mathbf{x}}_{k+1}+\mathbf{g}_{i_k,i_{k+1}} \tag{19e}$$

$$0\le T_1<T_2<\cdots<T_M \tag{19f}$$

$$\mathbf{x}_0=\mathbf{x}(0),\quad i_0=i(0) \tag{19g}$$

where $\mathbf{T}=[T_1,\ldots,T_M]^T$ and $\mathbf{I}=[i_1,\ldots,i_M]^T$. This cost looks much like the one in Xuping and Antsaklis (2003) and Seatzu et al. (2006), though here the average over time is taken and the state jump is governed by manoeuvres. Following Seatzu et al. (2006) it is easy to find symbolic expressions for $\overline{\mathbf{Q}}_i$, $\overline{\mathbf{r}}_i$, $\overline{s}_i$, $\overline{\mathbf{Q}}_{i,j}$, $\overline{\mathbf{r}}_{i,j}$, $\overline{s}_{i,j}$, $\overline{\mathbf{A}}_i$, $\overline{\mathbf{f}}_i$ as a function of the switching times, see Appendix A.

The ultimate goal would be to solve this problem for T approaching infinity while also allowing M to approach infinity. This is a hard, yet unsolved, problem for which reason the approximative solution described in Solberg, Andersen, and Stoustrup (2008) will be used. Hence set the number of switches equal to two $M=2$ and add the constraints $\mathbf{x}_2=\mathbf{x}_0$, $T=T_2+\delta T_{i_1,i_2}$ to find the optimal limit cycle if one exists.

Having found the optimal limit cycle and thereby found the two points $(\mathbf{x}^+,\mathbf{x}^-)$ representing the state just after each of the two switches, the switching surfaces and their domains can be calculated using techniques from time optimal control. Following Solberg, Andersen, and Stoustrup (2008) means starting by finding the solution to the system when the input is constant using the notation $x_1=p_s$, $x_2=u_f$, $u=\dot{m}_{fu}$, $\lambda_1=-1/\tau_{p_s}$, $\lambda_2=-1/a$, $f_1=(K_{p_s}/\tau_{p_s})(\dot{m}_{fu}-\dot{m}_{fu,ss})$, $f_2=\dot{m}_{fu}$, $\mathbf{x}^0=\mathbf{x}^-$, $\mathbf{x}=[x_1,x_2]^T$, $\mathbf{x}'=[x_1',x_2']^T$ and $\mathbf{\Lambda}=\left[\begin{smallmatrix}\lambda_1 & 0\\ 0 & \lambda_2\end{smallmatrix}\right]$.

$$\begin{bmatrix}x_1'(t)\\ x_2'(t)\end{bmatrix}=e^{\mathbf{\Lambda}t}\begin{bmatrix}x_1^0\\ x_2^0\end{bmatrix}+(e^{\mathbf{\Lambda}t}-1)\mathbf{\Lambda}^{-1}\begin{bmatrix}f_1\\ f_2\end{bmatrix} \tag{20}$$

Now the switching surface is sought which is a curve in the two-dimensional system. First find, Γ^-, the curve along which the state approach $\mathbf{x}^-$ with negative f_1 after a switch by setting $t=-\tau,(\tau>0)$ in (20) and eliminating τ. This curve is given by the equations:

$$\mathbf{x}'=\mathbf{M}_{1,2}\mathbf{x}+\mathbf{g}_{1,2} \tag{21a}$$

$$\tau(\mathbf{x}')=-\ln\left(\frac{x_1'+f_1/\lambda_1}{x_1^0+f_1/\lambda_1}\right)\Big/\lambda_1 \tag{21b}$$

$$f^-(\mathbf{x}')=\left(\frac{x_1'+f_1/\lambda_1}{x_1^0+f_1/\lambda_1}\right)^{\lambda_2/\lambda_1}-\left(\frac{x_2'+f_2/\lambda_2}{x_2^0+f_2/\lambda_2}\right)=0 \tag{21c}$$

over the domain $X_{\Gamma^-}=\{\mathbf{x}|\tau(\mathbf{x}')>0\}$. The curve Γ^+ and domain X_{Γ^+} can be found in a similar manner starting from the point $\mathbf{x}^+$. Now a new function describing the surface dividing the state space $E=\Gamma^+\cup\Gamma^-$ can be defined. This function, defined on $X_{\Gamma^+}\cup X_{\Gamma^-}$, is given as

$$f(\mathbf{x})=\begin{cases}f^+(\mathbf{x}) & \text{for } \mathbf{x}(t)\in X_{\Gamma^+}\\ f^-(\mathbf{x}) & \text{for } \mathbf{x}(t)\in X_{\Gamma^-}\end{cases} \tag{22}$$

Finally define the space above the surface E as E^- and the space below as E^+ being regions of the state space where a negative input or a positive input can take the state to one of the switching surfaces.

Now the switching law steering the state of the reduced order system to the optimal limit cycle is

$$u_b(t)=\begin{cases}1 & \text{for } \mathbf{x}(t)\in E^+\\ 0 & \text{for } \mathbf{x}(t)\in E^-\\ 1 & \text{for } \mathbf{x}(t)\in\Gamma^+\\ 0 & \text{for } \mathbf{x}(t)\in\Gamma^-\\ u_b(t) & \text{for } \mathbf{x}(t)\in\mathbb{R}^2\backslash(X_{\Gamma^+}\cup X_{\Gamma^-})\end{cases} \tag{23}$$

u_b can be either of the on signals to the two burners depending on the gap-region the power reference is belonging to. This law is implemented on the MPC + Logic level in the control structure in Fig. 5. It is obvious that the behaviour of this control law is close to that of ordinary hysteresis control, which would have one dimensional switching surfaces dependent on the pressure only. This is due to the system being of second order and the second state being simply a filtered version of the input. If one had chosen a cost where the integral of the pressure was penalised, a third order system would have been the result and a more complicated state trajectory would be the result.

Now this switching law is only valid for one particular u_{ss}. In practice the calculation in this section has to be done at every sample time of the outer controller to take account for the changing disturbance. However, it is also possible, as will be done here, to construct a look-up table by evaluating the optimal limit cycle off-line for as many different disturbance levels as the desired accuracy dictates and then use the switching surfaces which corresponds to the closest disturbance. This is computationally very efficient as evaluating the switching surfaces takes little resources whereas finding the optimal limit cycle is very demanding. The computational burden of the full controller implementation thus reduces to solving one QP, generation of constraint matrices for the QP's involving switches, finding state

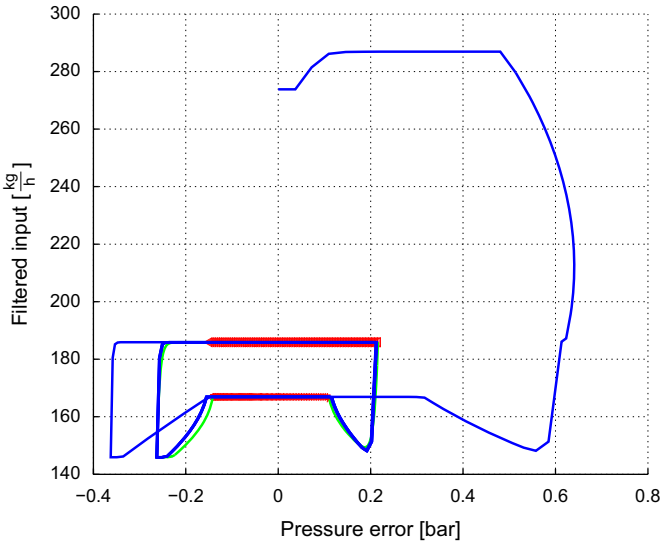

Fig. 6. Projection of the state trajectory into the plane containing p_s, u_f after a simulation on (4).

estimates, checking if the steam flow belongs to a gap-region by solving (9) and finally evaluating (23) if necessary.

An illustration of the method is shown in Fig. 6 where a simulation on the nonlinear model (4) has been carried out and the associate states (pressure and filtered fuel flow) are shown. The blue line is the state evolution while the red lines are the parts of the optimal limit cycle trajectory (for the linear system) between switches and the green lines the part during switches.

From this plot it can be seen that the state converges to a neighbourhood around the limit cycle. This indicates as assumed that the nonlinearities in the system are not pronounced in the fuel/pressure loop.

As the previous method based on finite horizon MPC this method is suboptimal. The suboptimality lies in the use of a reduced order model plus the separate optimisation of discrete and continuous decision variables in the outer and inner loop, respectively. Further, only a finite horizon cost is used when outside the gap-regions. However, this need not be the case as different methods exist for implementing quasi-infinite horizon strategies for linear systems (Mayne, Rawlings, Rao, & Scokaert, 2000). The horizon is set equal to the one for Method A.

4. Simulation results

This section presents simulation results applying the two methods discussed in Section 3 to the nonlinear simulation model of the marine boiler. The focus is directed to Gap-region 2 as this is the most interesting case regarding the sequences required to carry out a switch in Burner 2.

The simulation results for Method A are shown in the left column of Fig. 7. The disturbance profile used in the simulation is converted to represent the requested steam flow and is shown in the plot in row three column 1 as a red line. In the same plot the green line represents the estimated disturbance also converted into a presumed requested steam flow.

There are a few things to notice in this figure. The spikes in the fuel flow just after a burner switch from Mode 1 to Mode 2 are partly due to prediction mismatches. The problem is a large mismatch due to the blocking of switched inputs giving large differences in the predicted optimising input sequences from one sample to the next. Another problem is the short prediction horizon necessary to make the optimisation tractable. This implies that the algorithm will not take account of long term damage made by excessive input until it is too late. One could try adjusting the horizon length taking care not to make the horizon too long. In fact this method is very difficult to tune to achieve both good pressure and water level control using reasonable control signals. Also it is worth noticing the asymmetry in the pressure error oscillations when the disturbance corresponds to the gap-region. This stems from the manoeuvre necessary to perform during switches. When in Mode 1 and the maximum fuel input is injected a switch to Mode 2 requires the fuel input first to reach the minimum level for Mode 1. As weights are put on both the pressure error and input changes also during these manoeuvres it will naturally cost more to switch from Mode 1 to Mode 2 than the other way around. As the final performance included a weight on the pressure error and no weight on accumulated fuel use, this is not the desired performance. However, this could be compensated by e.g. using a cost for the integrated pressure error or by having asymmetric weights dependent on the current mode. However, such implementations are not standard and quite cumbersome for which reason the result presented above are used.

The simulation results for Method B are shown in the right column of Fig. 7. The lines in the plot in row three column two have the same interpretation as in the plot beside it and moreover the extra green line in the bottom right plot represents the estimated required steady state fuel flow.

As opposed to Method A the pressure error oscillations when in the gap-region are close to symmetric around the reference for Method B. The spikes in the fuel flow are also avoided using Method B. As can be seen it would be advantageous to reduce the uncertainty on the steam flow estimate as this is the key component in the method and too large variance on this can deteriorate performance. In particular, when close to the boundary of the gap-region the steady state estimate might switch between being outside and inside the gap-region. One natural possibility for reducing this phenomenon is to simply include a measurement of the steam flow instead of relying on an estimate. However, much of the performance lack for this estimate seems to come from the neglected nonlinearities in the low frequency region. The estimate converges when the pressure can reach a steady state but when the input saturates the pressure becomes "unstable" and the estimate seems to converge slowly. It would be simple to use different models dependent on the current load estimate which would be a natural extension to the presented approach. This is not done here in order to be able to compare the results from the two methods.

Regarding the water level control, only small oscillations are detected during burner on/off switching for both methods. Part of the original setup was not to improve pressure performance at the expense of water level regulation which has been achieved. The variation seems smaller though for Method B which is due to the sequential implementation which ensures that the water level control error is regulated to zero between burner switches.

5. Conclusion

Two different approaches to control a marine boiler equipped with a two-stage burner has been discussed: One, Method A, based on finite horizon MPC using a hybrid internal model and another, Method B, based on a generalised hysteresis approach. Both methods were able to provide satisfactory performance keeping both pressure and water level around the desired reference values. A direct performance comparison is difficult due to the heuristics involved in both methods. Even so there are

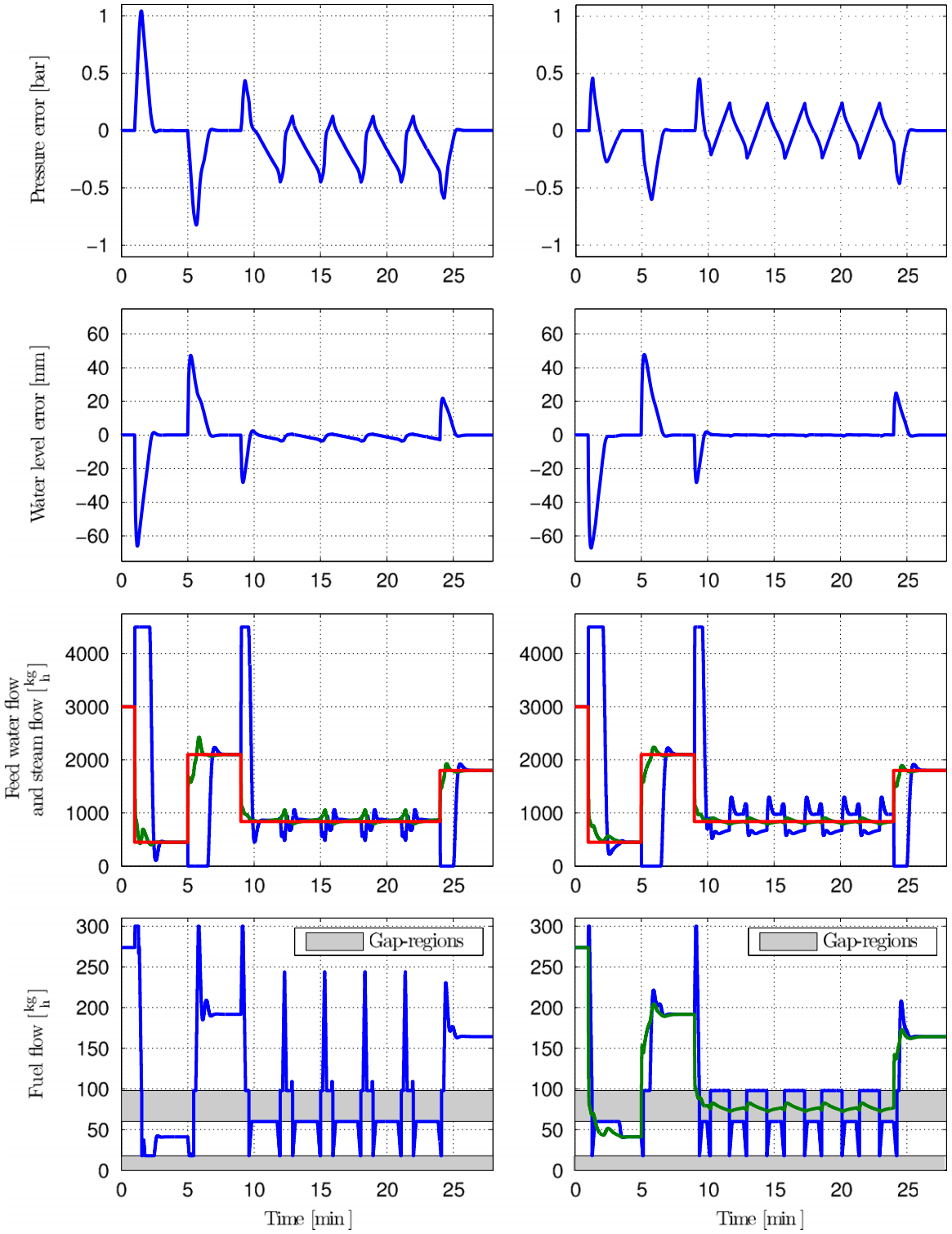

Fig. 7. Simulation results using Method A left and Method B right. From the top the first row shows pressure error, the second water level error, the third row shows the feed water flow (blue), estimated (green) and measured (red) disturbance both converted to represent requested steam flow, and the bottom row shows the fuel flow (blue) and to the right the estimated steady state fuel input (green). The gray fields in the bottom plots correspond to the gap-regions. Notice the spikes in the fuel flow from 12 to 25 min bottom left and the asymmetry in the pressure error oscillations in the same period top left for Method A.

still conclusions to be drawn regarding the choice of method. Recall that the objective of both methods was to minimise an infinite horizon cost and the performance weights were set equal.

Method B shows more acceptable fuel flows after burner switches and deliver a smaller variance for both pressure and water level control errors. The main reason for this is prediction mismatches related to Method A. Regarding Method B there is a risk of slow convergence as the ability to switch when the power request is just outside the gap is not utilised. This is naturally incorporated in Method A. Finally Method A proved very difficult to tune to achieve both good water level and pressure performance which did not seem to be the case for Method B.

Both of the proposed methods are suboptimal solutions of the original control problem. Further both methods requires optimisation solvers to be shipped with the industrial product. Regarding off-line design Method B requires considerably more computations for finding switching surfaces related to the hysteresis. However, as the size of QP's and constraint matrices are comparable and evaluating the switching law for Method B is fast, the main difference in the on-line computational burden for the two methods lies in the number of QP's solved at each sample time. Method A has a worst case of five QP's to solve at each sample time while Method B has only one.

Method B has the advantage that it can easily be reduced to a conventional hysteresis controller. The method is relevant also for normal boilers running on/off burner control and can be used for finding conventional hysteresis bounds. Further the continuous controller needs not be MPC type but can be replaced by any suitable controller of the designer's choice. The method is not limited to burner control but can be applied with advantage in all systems in which the actuator signal is characterised as being continuous over one region and discrete outside this region.

Acknowledgement

The authors are grateful for the support provided by Aalborg Industries A/S during the preparation of this paper.

Appendix A. Construction of matrices for optimisation problem

This appendix describes how to construct the matrices used to define the optimisation problem (19), with relation to model (17) and manoeuvres (18):

$$\overline{\mathbf{A}}_i(\delta) = e^{\mathbf{A}_i\delta} \tag{A.1a}$$

$$\overline{\mathbf{f}}_i(\delta) = e^{\mathbf{A}_i\delta}\int_0^\delta e^{-\mathbf{A}_i\tau}\mathbf{f}_i(\tau)\,d\tau \tag{A.1b}$$

and allowing a cost on the input $\mathbf{u}^T\mathbf{S}_i\mathbf{u}$ for generality leads to

$$\overline{\mathbf{Q}}_i(\delta) = \int_0^\delta e^{\mathbf{A}_i^T t}\mathbf{C}_i^T\mathbf{Q}_i\mathbf{C}_i e^{\mathbf{A}_i t}\,dt \tag{A.2a}$$

$$\overline{\mathbf{r}}_i(\delta) = 2\int_0^\delta e^{\mathbf{A}_i^T t}\mathbf{C}_i^T\mathbf{Q}_i\left(\mathbf{C}_i e^{\mathbf{A}_i t}\left(\int_0^t e^{-\mathbf{A}_i\tau}\mathbf{f}_i(\tau)\,d\tau\right)+\mathbf{D}_i\mathbf{u}_i(t)\right)dt \tag{A.2b}$$

$$\begin{aligned}\overline{s}_i(\delta) = \int_0^\delta \Big\{ &\mathbf{u}_i(t)^T(\mathbf{D}_i^T\mathbf{Q}_i\mathbf{D}_i+\mathbf{S}_i)\mathbf{u}_i(t)\\ &+2\mathbf{u}_i(t)^T\mathbf{D}_i^T\mathbf{Q}_i\mathbf{C}_i e^{\mathbf{A}_i t}\left(\int_0^t e^{-\mathbf{A}_i\tau}\mathbf{f}_i(\tau)\,d\tau\right)\\ &+\left(\int_0^t \mathbf{f}_i^T(\tau)e^{-\mathbf{A}_i^T\tau}\,d\tau\right)e^{\mathbf{A}_i^T t}\mathbf{C}_i^T\mathbf{Q}_i\mathbf{C}_i e^{\mathbf{A}_i t}\left(\int_0^t e^{-\mathbf{A}_i\tau}\mathbf{f}_i(\tau)\,d\tau\right)\Big\}\,dt\end{aligned} \tag{A.2c}$$

If $\mathbf{A}_i$ is Hurwitz, $\mathbf{D}_i=0$, $\mathbf{S}_i=0$ and $\mathbf{f}_i=0$:

$$\overline{\mathbf{Q}}_i(\delta) = \mathbf{Z}_i - e^{\mathbf{A}_i^T\delta}\mathbf{Z}_i e^{\mathbf{A}_i\delta},\quad \overline{\mathbf{r}}_i(\delta)=0,\quad \overline{s}_i(\delta)=0 \tag{A.3}$$

where $\mathbf{Z}_i$ is the solution to the Lyapunov equation $\mathbf{A}_i^T\mathbf{Z}_i+\mathbf{Z}_i\ \mathbf{A}_i=-\mathbf{C}_i^T\mathbf{Q}_i\mathbf{C}_i$. Instead if the assumption on $\mathbf{A}_i$ is that it is diagonisable, $\mathbf{A}_i=\mathbf{V}_i\mathbf{\Lambda}_i\mathbf{V}_i^{-1}$, where $\mathbf{\Lambda}_i=\mathrm{diag}(\lambda_1,\ldots,\lambda_n)$, then

$$\overline{\mathbf{Q}}_i(\delta) = (\mathbf{V}_i^{-1})^T\left(\int_0^\delta e^{\mathbf{\Lambda}_i^T t}\mathbf{V}_i^T\mathbf{C}_i^T\mathbf{Q}_i\mathbf{C}_i\mathbf{V}_i e^{\mathbf{\Lambda}_i t}\,dt\right)\mathbf{V}_i^{-1} \tag{A.4a}$$

$$\overline{\mathbf{r}}_i(\delta) = 2(\mathbf{V}_i^{-1})^T\int_0^\delta\left\{e^{\mathbf{\Lambda}_i^T t}\mathbf{V}_i^T\mathbf{C}_i^T\mathbf{Q}_i\left(\mathbf{C}_i\mathbf{V}_i e^{\mathbf{\Lambda}_i t}\left(\int_0^t e^{-\mathbf{\Lambda}_i\tau}\mathbf{V}_i^{-1}\mathbf{f}_i(\tau)\,d\tau\right)+\mathbf{D}_i\mathbf{u}_i(t)\right)\right\}dt \tag{A.4b}$$

$$\begin{aligned}\overline{s}_i(\delta) = \int_0^\delta \Big\{ &\mathbf{u}_i(t)^T(\mathbf{D}_i^T\mathbf{Q}_i\mathbf{D}_i+\mathbf{S}_i)\mathbf{u}_i(t)+2\mathbf{u}_i(t)^T\mathbf{D}_i^T\mathbf{Q}_i\mathbf{C}_i\mathbf{V}_i e^{\mathbf{\Lambda}_i t}\left(\int_0^t e^{-\mathbf{\Lambda}_i\tau}\mathbf{V}_i^{-1}\mathbf{f}_i(\tau)\,d\tau\right)\\ &+\left(\int_0^t \mathbf{f}_i^T(\tau)(\mathbf{V}_i^{-1})^T e^{-\mathbf{\Lambda}_i^T\tau}\,d\tau\right)e^{\mathbf{\Lambda}_i^T t}\mathbf{V}_i^T\mathbf{C}_i^T\mathbf{Q}_i\mathbf{C}_i\mathbf{V}_i e^{\mathbf{\Lambda}_i t}\left(\int_0^t e^{-\mathbf{\Lambda}_i\tau}\mathbf{V}_i^{-1}\mathbf{f}_i(\tau)\,d\tau\right)\Big\}\,dt\end{aligned} \tag{A.4c}$$

These integrals are easy to calculate symbolically due to the simple form of the matrix exponential of a diagonal matrix. Further,

$$H_{i,j}(\tilde{\mathbf{x}}_k) = \sum_{h=0}^{N-1}[\mathbf{x}_h^T\overline{\mathbf{Q}}_{i_h}(\tau_{h+1})\mathbf{x}_h+\mathbf{x}_h^T\overline{\mathbf{r}}_{i_h}(\tau_{h+1})+\overline{s}_{i_h}(\tau_{h+1})], \tag{A.5}$$

with

$$\mathbf{x}_{h+1} = e^{\mathbf{A}_{i_h}\tau_{h+1}}\mathbf{x}_h + e^{\mathbf{A}_{i_h}\tau_{h+1}}\int_0^{\tau_{h+1}} e^{-\mathbf{A}_{i_h}\tau}\mathbf{f}_{i_h}(\tau)\,d\tau \tag{A.6a}$$

$$\mathbf{x}_0 = \tilde{\mathbf{x}}_k \tag{A.6b}$$

with N being the number of continuous input profiles that make up the manoeuvre and τ_j the time spent with input profile u_{j-1}. By defining $\tilde{\mathbf{Q}}_{i,j}=\mathrm{diag}(\mathbf{Q}_{i_0}(\tau_1),\ldots,\mathbf{Q}_{i_{N-1}}(\tau_N))$, $\tilde{\mathbf{r}}_{i,j}^T=[\mathbf{r}_{i_0}(\tau_1)^T,\ldots,\mathbf{r}_{i_{N-1}}(\tau_N)^T]$ and $\tilde{s}_{i,j}=s_{i_0}(\tau_1)+\cdots+s_{i_{N-1}}(\tau_N)$, (A.5) can be rewritten as a quadratic form in $\tilde{\mathbf{x}}_k$

$$H_{i,j}(\tilde{\mathbf{x}}_k) = \tilde{\mathbf{x}}_k^T\underbrace{\overline{\mathbf{M}}_{i,j}^T\tilde{\mathbf{Q}}_{i,j}\overline{\mathbf{M}}_{i,j}}_{\overline{\mathbf{Q}}_{i,j}}\tilde{\mathbf{x}}_k+\tilde{\mathbf{x}}_k^T\underbrace{\overline{\mathbf{M}}_{i,j}^T(2\tilde{\mathbf{Q}}_{i,j}\overline{\mathbf{g}}_{i,j}+\tilde{\mathbf{r}}_{i,j})}_{\overline{\mathbf{r}}_{i,j}}+\underbrace{\overline{\mathbf{g}}_{i,j}^T\tilde{\mathbf{Q}}_{i,j}\overline{\mathbf{g}}_{i,j}+\overline{\mathbf{g}}_{i,j}^T\tilde{\mathbf{r}}_{i,j}+\tilde{s}_{i,j}}_{\overline{s}_{i,j}} \tag{A.7}$$

where

$$\begin{aligned}\begin{bmatrix}\mathbf{x}_0\\ \mathbf{x}_1\\ \mathbf{x}_2\\ \vdots\\ \mathbf{x}_{N-1}\end{bmatrix} &= \begin{bmatrix}\mathbf{I}\\ e^{(\mathbf{A}_1\tau_1)}\\ e^{(\mathbf{A}_1\tau_1+\mathbf{A}_2\tau_2)}\\ \vdots\\ e^{\left(\sum_{n=1}^{N-1}\mathbf{A}_n\tau_n\right)}\end{bmatrix}\tilde{\mathbf{x}}_k\\ &+\begin{bmatrix}\mathbf{0} & \mathbf{0} & & \\ e^{\mathbf{A}_1\tau_1} & \mathbf{0} & & \\ e^{(\mathbf{A}_1\tau_1+\mathbf{A}_2\tau_2)} & e^{\mathbf{A}_2\tau_2} & & \\ & \vdots & \ddots & \\ e^{\left(\sum_{n=1}^{N-1}\mathbf{A}_n\tau_n\right)} & & e^{\left(\sum_{n=2}^{N-1}\mathbf{A}_n\tau_n\right)} & \cdots\ e^{\mathbf{A}_{N-1}\tau N-1}\end{bmatrix}\\ &\times\begin{bmatrix}\int_0^{\tau_1} e^{-\mathbf{A}_1\tau}\mathbf{f}_1(\tau)\,d\tau\\ \int_0^{\tau_2} e^{-\mathbf{A}_2\tau}\mathbf{f}_2(\tau)\,d\tau\\ \vdots\\ \int_0^{\tau_{N-1}} e^{-\mathbf{A}_{N-1}\tau}\mathbf{f}_{N-1}(\tau)\,d\tau\end{bmatrix}\end{aligned} \tag{A.8a}$$

$$\overline{\mathbf{x}} = \overline{\mathbf{M}}_{i,j}\tilde{\mathbf{x}}_k+\overline{\mathbf{g}}_{i,j} \tag{A.8b}$$

where for simplicity $i_0=1$, $i_1=2,\ldots$ have been used.

References

Åström, K. J., & Bell, R. D. (2000). Drum boiler dynamics. *Automatica*, *36*, 363–378.

Bemporad, A., Giua, A., & Seatzu, C. (2002). A master–slave algorithm for the optimal control of continuous-time switched affine systems. In *Proceedings of the IEEE conference on decision and control* (Vol. 2, pp. 1976–1981).

Bemporad, A., & Morari, M. (1999). Control of systems integrating logic, dynamics, and constraints. *Automatica*, *35*, 407–427.

Cheng, K., Bentsman, J., & Taft, C. W. (2008). Full operating range robust hybrid control of a coal-fired boiler/turbine unit. *Journal of Dynamic Systems, Measurements and Control*, *130*, 041011-1–041011-14.

Frazzoli, E. (2001). *Robust hybrid control for autonomous vehicle motion planning*. Ph.D. thesis, MIT, June.

Frazzoli, E., Dahleh, M., & Feron, E. (1999). A hybrid control architecture for aggressive maneuvering of autonomous helicopters. In *Proceedings of the 38th IEEE conference on decision and control* (Vol. 3, pp. 2471–2476), December.

Giua, A., Seatzu, C., & Van der Mee, C. (2001). Optimal control of autonomous linear systems switched with a pre-assigned finite sequence. In *IEEE international symposium on intelligent control—proceedings* (pp. 144–149).

Hedlund, S., & Rantzer, A. (1999). Optimal control of hybrid systems. In *Proceedings of the 38th IEEE conference on decision and control* (Vol. 4, pp. 3972–3977).

Keshavarz, M., Barkhordary, M., & Motlagh, M. R. J. (2007). Mixed logic dynamical modeling and control of steam boiler. In *International conference on control, automation and systems*.

Kothare, M. V., Mettler, B., Morari, M., Bendotti, P., & Falinower, C.-M. (2000). Level control in the steam generator of a nuclear power plant. *IEEE Transactions on Control System Technology*, *8*(1), 55–69.

Kvasnica, M., Grieder, P., & Baotić, M. (2004). *Multi-parametric toolbox* (MPT). URL ⟨http://control.ee.ethz.ch/∼mpt⟩.

Lee, Y. S., Kwon, W. H., & Kwon, O. K. (2000). A constrained receding horizon control for industrial boiler systems. In G. Hencsey (Ed.), *IFAC symposium on manufacturing, modeling, management and control* (*MIM 2000*) (pp. 411–416), Patras, Greece.

Maciejowski, J. M. (2001). *Predictive control with constraints*. Harlow: Pearson Education Limited.

Mayne, D. Q., Rawlings, J. B., Rao, C. V., & Scokaert, P. O.M. (2000). Constrained model predictive control: Stability and optimality. *Automatica*, *36*(6), 789–814.

Mortensen, J. H., Mølbak, T., Andersen, P., & Pedersen, T. S. (1998). Optimization of boiler control to improve the load-following capability of power-plant units. *Control Engineering Practice*, *6*, 1531–1539.

Pannocchia, G., & Rawlings, J. B. (2003). Disturbance models for offset-free model-predictive control. *American Institute of Chemical Engineers, AIChE*, *49*, 426–437.

Rossiter, J., Neal, P., & Yao, L. (2002). Applying predictive control to a fossil-fired power station. *Transactions of the Institute of Measurement and Control*, *24*, 177–194.

Rossiter, J. A. (2003). *Model-based predictive control: A practical approach*. CRC Press LLC.

Sarabia, D., de Prada, C., Cristea, S., & Mazaeda, R. (2005). Hybrid model predictive control of a sugar end section. In *European symposium on computer aided process engineering*, *ESCAPE* 16, 2000 N.W. Corporate Blvd., Boca Raton, Florida 33431.

Seatzu, C., Corona, D., Giua, A., & Bemporad, A. (2006). Optimal control of continuous-time switched affine systems. *IEEE Transactions on Automatic Control*, *51*(5), 726–741.

Solberg, B., Andersen, P., Maciejowski, J. M., & Stoustrup, J. (2008). Hybrid model predictive control applied to switching control of burner load for a compact marine boiler design. In D. D. Cho (Ed.), *17th IFAC World congress*, Seoul, Korea.

Solberg, B., Andersen, P., & Stoustrup, J. (2007). *Advanced water level control in a one-pass smoke tube marine boiler*. Technical Report, Department of Electronic Systems, Aalborg University, Aalborg, Denmark.

Solberg, B., Andersen, P., & Stoustrup, J. (2008). Optimal switching strategy for systems with discrete inputs using a discontinuous cost functional, International Journal of Control, March, submitted for publication.

Solberg, B., Karstensen, C. M.S., & Andersen, P. (2007). Control properties of bottom fired marine boilers. *Energy*, *32*, 508–520.

Solberg, B., Karstensen, C. M. S., Andersen, P., Pedersen, T. S., & Hvistendahl, P. U. (2005). Model-based control of a bottom fired marine boiler. In: P. Horacek (Ed.), *16th IFAC World congress*, Prague, Czech Republic.

Torrisi, F. D., & Bemporad, A. (2004). Hysdel—A tool for generating computational hybrid models for analysis and synthesis problems. *IEEE Transactions on Control Systems Technology*, *12*, 235–249.

Xuping, X., & Antsaklis, P., 2003. Quadratic optimal control problems for hybrid linear autonomous systems with state jumps. In *Proceedings of the American control conference* (Vol. 4, pp. 3393–3398).

Zhao, H., Li, W., Taft, C., & Bentsman, J. (1999). Robust controller design for simultaneous control of throttle pressure and megawatt output in a power plant unit. *International Journal of Robust and Nonlinear Control*, *9*, 425–446.